A Microscopic and Spectroscopic Study of Interactions between Carbon Nanotubes and a Conjugated Polymer

ARTICLE *in* THE JOURNAL OF PHYSICAL CHEMISTRY B · FEBRUARY 2002

Impact Factor: 3.3 · DOI: 10.1021/jp013745f

13 AUTHORS, INCLUDING:

Alan B Dalton
University of Surrey
119 PUBLICATIONS **5,228** CITATIONS
SEE PROFILE

Hugh J Byrne
Dublin Institute of Technology
294 PUBLICATIONS **5,709** CITATIONS
SEE PROFILE

David Carroll
Wake Forest University
264 PUBLICATIONS **10,362** CITATIONS
SEE PROFILE

Werner J Blau
Trinity College Dublin
565 PUBLICATIONS **16,868** CITATIONS
SEE PROFILE

A Microscopic and Spectroscopic Study of Interactions between Carbon Nanotubes and a Conjugated Polymer

B. McCarthy,[†] J. N. Coleman,*[,†] R. Czerw,[‡] A. B. Dalton,[§] M. in het Panhuis,[†] A. Maiti,[||] A. Drury,[†] P. Bernier,[⊥] J. B. Nagy,[#] B. Lahr,[†] H. J. Byrne,[¶] D. L. Carroll,[‡] and W. J. Blau[†]

Materials Ireland Polymer Research Centre, Department of Physics, Trinity College Dublin, Dublin 2, Ireland, Department of Physics and Astronomy, Clemson University, Clemson, South Carolina 29634, University of Texas at Dallas, NanoTech Institute, Richardson, Texas 75080, Accelrys Inc., 9685 Scranton Road, San Diego, California 92121-3752, Groupe de Dynamique des Phases Condensées, Université de Montpellier II, 34095 Montpellier cedex 05, France, Laboratoire de Résonance Magnétique Nucléaire, Facultes Universitaires Notre Dame de la Paix, rue de Bruxelles 61, 5000 Namur, Belgium, and Facility for Optical Characterization and Spectroscopy/School of Physics, Dublin Institute of Technology, Kevin St., Dublin 8, Ireland

Received: October 9, 2001; In Final Form: December 7, 2001

Production of stable polymer−nanotube composites depends on good wetting interaction between polymer and nanotube, which is polymer specific, and depends in particular on chain conformation. In this paper, we examine this interaction for a conjugated, semiconducting polymer by a range of microscopic and spectroscopic techniques, to gain a greater understanding of the binding. Several interesting effects are observed, including an order to the interaction between the polymer and nanotube, the tendency of defects in the nanotube structure to nucleate crystal growth, and substantial changes in the spectroscopic behavior of the polymer due to the effect of the nanotubes on polymer conformation. This is substantiated by computational modeling, which demonstrates that these conformational modifications are due to the interaction with the nanotubes.

1. Introduction

The unique electronic and mechanical properties of nanotubes[1] have promised much potential for a vast range of applications, including quantum wires,[2] tips for scanning probe microscopy,[3] and molecular diodes.[4] Recently, much attention has been given to the use of nanotubes in composite materials, to harness their exceptional mechanical[5] and electronic[6,7] properties. A wide range of host materials have been used, including polymers,[8,9] ceramics,[10] and metals.[11] Research[12] here in Trinity has focused on composites of electronically active conjugated polymers and carbon nanotubes, which demonstrate a number of advantages. Conjugated polymers show potential for electronic device applications[13] with the incorporation of carbon nanotubes promising to greatly enhance transport properties in these systems.[14] This is thought to be a key issue for the realization of viable devices such as organic light-emitting diodes (OLEDS). Furthermore, incorporation of nanotubes should also increase the mechanical properties of composite materials[15] and, by increasing their thermal conductivity, improve environmental stability.[12] In addition, during composite formation the problems of nanotube purity and processing are also addressed due to the selective dispersion of nanotubes in the polymer matrix. While conjugated polymers are known to coat both nanotubes and graphitic impurities, only the polymer-coated nanotubes form a stable dispersion with the impurities sedimenting out of solution. This allows the subsequent purification of the composite by decantation. This completely nondestructive purification method has been very successful with 50−70% of the available nanotubes remaining in solution.[16] In comparison, less than 5% of the impurities are dispersed.[17] This is desirable as most alternative purification methods depend on either filtration[18] or oxidation,[19] which have the disadvantages of low yield and the modification of the nanotubes.

In this paper, this interaction between the conjugated polymer and nanotubes is characterized by Transmission Electron Microscopy (TEM), Scanning Tunneling Microscopy (STM), and optical and Raman spectroscopy. Computational modeling of PmPV−SWNT systems is also presented to clarify these observations. Excellent wetting of the nanotubes by the polymer is observed, demonstrating considerable polymer−nanotube interaction. Results also suggest a mapping of the polymer onto the nanotube surface, resulting in substantial alteration of the polymer's electronic structure. This is manifested by modifications to the spectroscopic properties of PmPV, due to the induced conformational changes. Computational modeling agrees with this, and serves to further clarify this interaction.

2. Experimental Details

The conjugated polymer used is poly(*m*-phenylenevinylene-*co*-2,5-dioctyloxy-*p*-phenylenevinylene), (PmPV).[20] Three types of carbon nanotubes are used: Multiwalled Nanotubes[21] (MWNT) made by the Arc Discharge Method,[22] Arc Discharge Method Single-Walled Nanotubes[23] (SWNT), and MWNT made by catalytic decomposition of acetylene.[24] To prepare composites of these materials is relatively simple; a solution of PmPV in toluene is made (typically ∼1 g/L), and to this the required mass

* Author to whom correspondence should be addressed.
[†] Trinity College.
[‡] Clemson University.
[§] University of Texas at Dallas, NanoTech Institute.
[||] Accelrys Inc.
[⊥] Université de Montpellier II.
[#] Laboratoire de Résonance Magnétique Nucléaire, Facultes Universitaires Notre Dame de la Paix.
[¶] Dublin Institute of Technology.

10.1021/jp013745f CCC: $22.00
Published on Web 02/08/2002

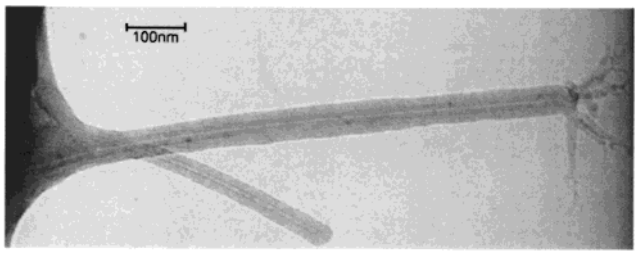

Figure 1. TEM of two coated MWNT protruding from the film edge. Note the dendritic polymer growths on the end of one of the nanotubes.

fraction of nanotubes is added prior to sonication. SWNT composites tend to saturate at 1−2% nanotube content as the excess nanotubes aggregate. However, this excess can be decanted off, leaving a well-dispersed PmPV/SWNT solution. As a much higher mass fraction of MWNT than SWNT can be dispersed in a PmPV solution, MWNT composites of very high mass fraction can be readily made.

To prepare these composites for TEM, grids (both holey carbon, and Formvar-coated copper grids are used) are partially dipped into a dilute composite solution. These are then allowed to dry in air. It is then relatively easy to find examples of PmPV-coated nanotubes at film edges. For STM, a small amount of dilute composite solution is pipetted onto Highly Oriented Pyrolytic Graphite (HOPG), then allowed to dry in a vacuum, and transferred into the STM chamber. Spectroscopic measurements are carried out in solid state, where the composite is spun-cast from solution onto Spectrosil B disks.

3. Results

3.1. Transmission Electron Microscopy. Examining MWNT composites, a range of interesting phenomena can be observed. Figure 1 shows two PmPV-coated arc discharge method nanotubes protruding from the edge of the composite film. The nanotubes are visible as the darker region at the center of these fibers, with the hollow core of the nanotube being visible within. It can be seen that the PmPV coating is approximately 25 nm thick. This is indicative of good binding in the composite, as each nanotube supports quite a considerable mass of PmPV.

On the tip of the longer nanotube, it can be seen that there are five crystalline growths of PmPV. This, and another example observed in a catalytically grown nanotube sample, are shown in greater detail in Figure 2. The growths are quite large, extending for approximately 200 nm in total. A further example of these dendritic polymer growths is presented in Figure 3 A. It can be seen that there are approximately twenty growths from the nanotube body. The nanotubes in this particular composite are catalytically grown, and, as observed elsewhere, tend to have a large number of defects, which induce localized bends in the nanotube body. While defects cannot be directly observed, their positions can be determined in some cases by the location of these bends, and, in these cases, there is an excellent correspondence between the defects and the polymeric growths. The growths become more frequent toward the tip, agreeing well with the fact that the frequency of defect-induced bends in the growth axis increases toward the tip as observed in other TEM studies.[24] Furthermore, by examining Figure 2B, it can be seen that the dendrites correspond with the regions of greatest curvature of the tip where the defects necessary for closure most probably lie.

This PmPV derivative has been shown to be partially crystalline (∼30%),[20] so it is likely that, given a suitable nucleation site, it will form nano-crystallites as it precipitates from solution. Defects evidently offer such a nucleation site,

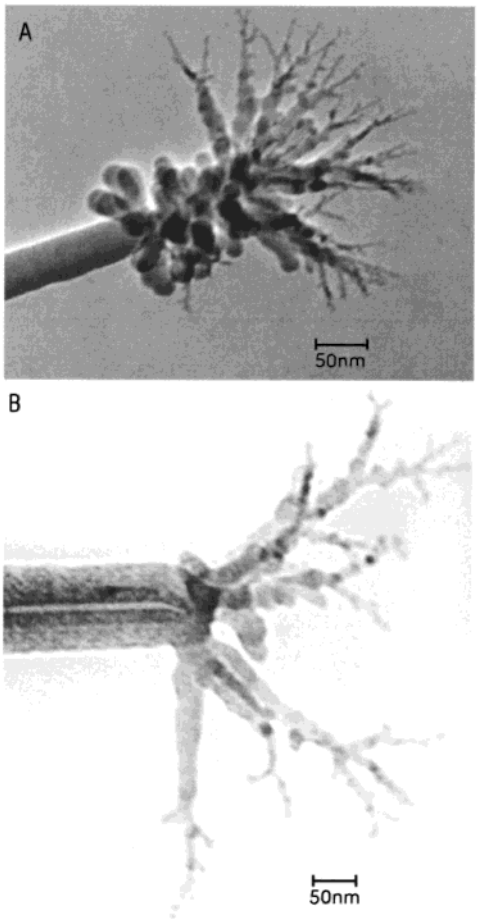

Figure 2. (A) Further example of dendritic growth, in a catalytically grown nanotube. (B) Magnified view of tip shown in Figure 1.

probably due to the increased charge localization accompanying these stuctures.[25]

Figure 3B demonstrates another interesting feature of this composite system. It shows a catalytically grown nanotube with a thin PmPV coating. It can clearly be seen that there is an apparently organization in the coating, giving an indication that there might be an order to the interaction between the nanotube and the PmPV. Several more conclusive examples of this are observed in the SWNT samples, by both STM and TEM, and will be analyzed in further detail later.

Shown in Figure 4A is a TEM of a SWNT network coated in PmPV, consisting of a large amount of intertwined PmPV-coated ropes. The diameter of these large fibers is in the range 70−120 nm. Given this large diameter relative to the size of SWNT (typically ∼1 nm), it is clear that there must be an extremely heavy coating of PmPV on this fiber. This is clearly observed in some of the fibers toward the top left, where lighter central regions can be observed. These are due to ropes of SWNT within the fibers. The diameters of the observable ropes are in the range 6−12 nm, suggesting that these are ropes consisting of 20−80 SWNT.

Another feature of this image worth noting is the cylindrically symmetrical coating of the nanotube on the bottom left. Also of interest are the ordered variations in diameter of the wrapping, from 106 nm at its widest point tapering to 40 nm at its narrowest. The wrapping is also at a slight angle to the cylindrical axis, measured at approximately 7°, varying by 2−3° over the length of the structure.

Compared to the other fibers, which are relatively unstructured and uniform, this particular fiber shows remarkable order

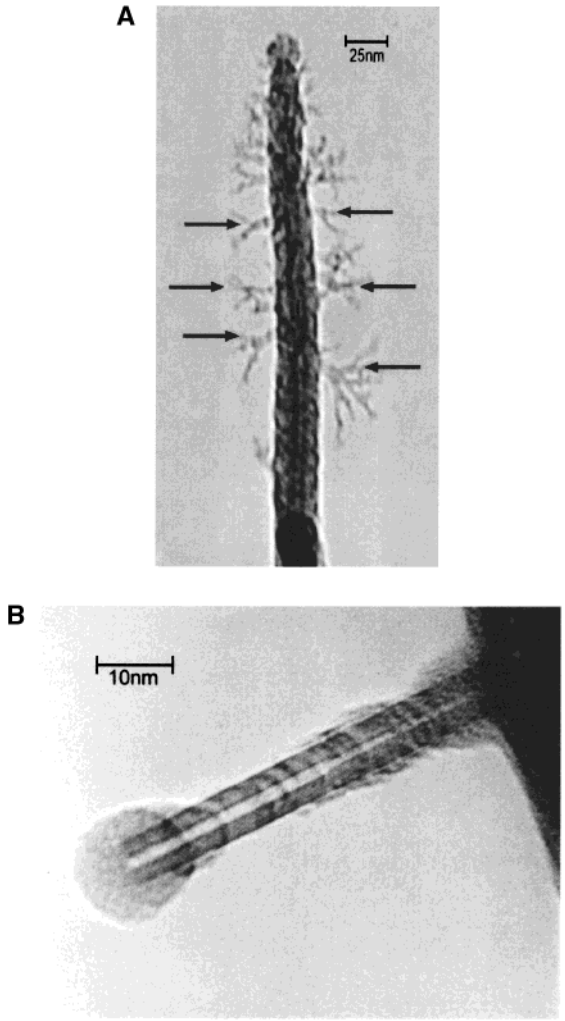

Figure 3. (A) A catalytically grown nanotube, with numerous dendritic growths. Arrows indicate obvious bends in the nanotube, where crystalline growth is nucleated. (B) TEM of catalytically grown nanotube, showing a highly ordered PmPV coating.

and structure. The angular orientation to the cylindrical axis suggests that there is some underlying symmetry within this fiber, for the PmPV to crystallize onto. This suggests the hypothesis that, unlike the uniform fibers where ropes can clearly be seen, this fiber contains an individual SWNT, suggesting some correlation between the nanotube lattice structure and the PmPV coating. This may explain the angular orientation of the coating, which could be determined by the nanotube's chiral angle. It is also consistent with the marked difference between this example and the uniformly coated fibers of SWNT ropes observed elsewhere in this image. Higher magnification TEM is unable to resolve any SWNT core to this structure. This is to be expected given the microscope's resolution. Observation of these examples is corroborated by STM, in relation to which these features are further discussed.

3.2. Scanning Tunneling Microscopy. While studying nanotubes using a HOPG substrate, care must be taken as HOPG fibers and steps are common, which exhibit long-range periodicity and are of similar dimensions to nanotubes.[26,27] However, nanotubes do appear substantially different and the electronic structure of PmPV-coated nanotube fibers here provides conclusive proof that these are not HOPG artifacts.

Shown in Figure 4B are two such fibers lying on the HOPG substrate. For convenience, the coated SWNTs on the left and right will be referred to as SWNT #1 and SWNT #2,

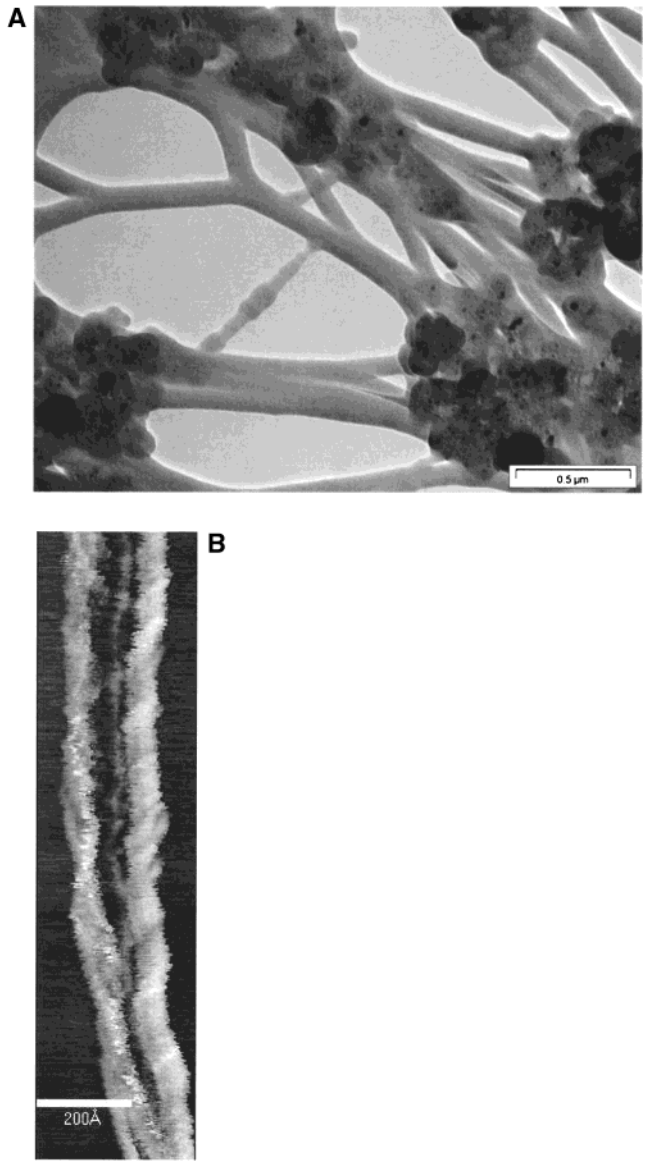

Figure 4. (A) TEM image of a SWNT composite. Note the light central regions in many of the fibers, indicating the presence of SWNT ropes, and the symmetrically coated SWNT in the foreground. (B) Image of two PmPV-coated SWNT lying on HOPG. Nanotube on left - SWNT #1, nanotube on right - SWNT #2. Note the ordered coating around SWNT #2. SWNT #1 consists of two individual tubes. Note how they separate at the bottom of the figure.

respectively. SWNT #1 is observed to have a pronounced helicity toward the lower part of the image. SWNT #2 does not have this helicity although there is a noticeable order in the PmPV coating, characterized by parallel lines at a constant angle of $19 \pm 2°$ between the coating and the nanotube diameter throughout its length. Note the similarity between this oriented wrapping and the example observed by TEM in Figure 4A.

Cross-sectional analysis yields the height of SWNT #1 as 15 Å including coating, although its profile is irregular. In contrast, the height of coated SWNT #2 is approximately 20 Å. It is well-known that tip convolution effects exaggerate measurements in the plane resulting in the discrepancy between the measured nanotube widths and heights. A PmPV oligomer with the same dioctyloxy sidegroups has been calculated to stack with an interlayer distance of 3.5 Å.[28] Therefore, these SWNTs are coated with only 1−2 layers of PmPV. Due to the polymer coating the diameters of the nanotubes cannot be determined exactly by topographic analysis. However, they can be ascer-

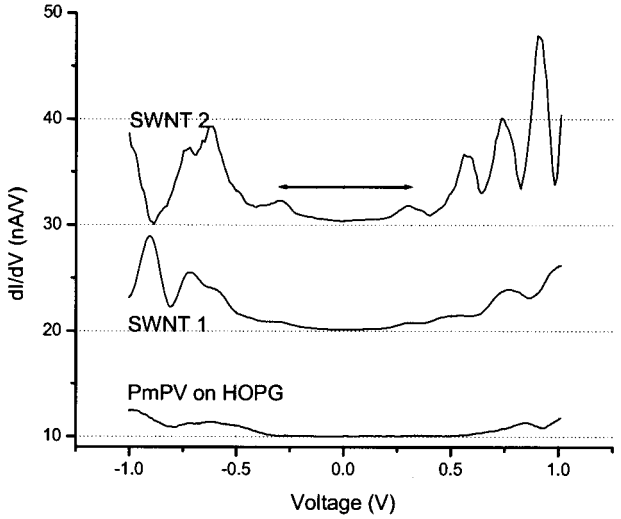

Figure 5. LDOS of SWNT #1 and SWNT #2, with PmPV on HOPG as a reference. The sharp peaks in the SWNT LDOS indicate the location of van Hove singularities.

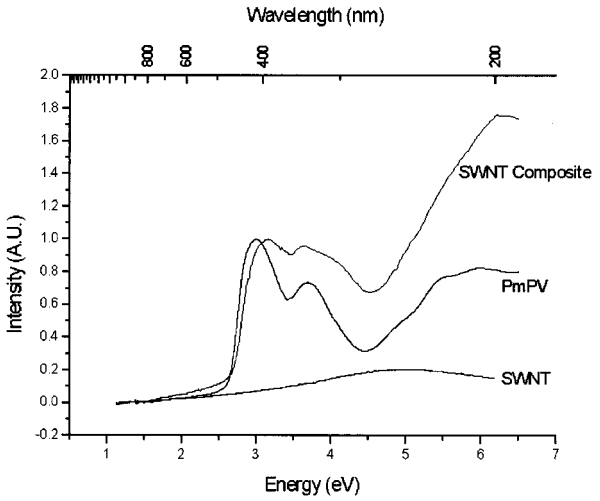

Figure 6. UV−visible absorption of composite, PmPV, and SWNT. The effect of the SWNT is to blue-shift the spectrum and shift the dominant absorption to higher energies.

tained by examining the positions of the van Hove singularities in the local density of states (LDOS) of the nanotubes.[6,7] The spacing between these peaks is determined by the diameter of the SWNT via the relation,[29] $E(\text{eV}) = 0.7668/d(\text{nm})$.

The LDOS of these nanotubes in the −1.0 to 1.0 eV region as measured by scanning tunneling spectroscopy (offset for clarity), are presented in Figure 5 The dominant contribution to these LDOS are the nanotubes, as the PmPV is relatively featureless in this region.[30] The characteristic singularities are apparent as the sharp, regularly spaced features. A line denotes the separation between the first van Hove singularities.

From the LDOS of SWNT #2, it can be seen that the separation between the first van Hove singularities is 0.6 eV, implying a diameter of 1.28 nm, supporting the earlier suggestion that the PmPV coating is no more than one or two layers.

For the PmPV coating to show such regularity over its length, it is reasonable to expect that the coating would be reflective of the underlying SWNT symmetries, with the angle of coating (19°) corresponding to the SWNT's chiral angle. This hypothesis is strengthened by the previous observation by TEM of a similar coating, but at a much different angle of 7°, demonstrating that this orientation does vary with the underlying nanotube. Thus, this is not just a phenomenon of PmPV structure, but must be due to the underlying lattice structure of the nanotube.

From this, we can estimate the chirality of this SWNT, as both diameter (1.28 nm) and chiral angle (19 ± 2°) are solely determined by the roll-up vector of the SWNT.[29] Examining all possible (n,m) values, and allowing a degree of tolerance in these measured values, two types of SWNT could plausibly account for these measurements. One is a (13,6) nanotube ($d = 1.31$ nm, $E = 0.58$ eV, $\theta = 18.0°$); the other is a (12,7) nanotube ($d = 1.30$ nm, $E = 0.59$ eV, $\theta = 21.4°$). There is very little to differentiate between these SWNTs in their physical characteristics.

Similarly, the band gap of SWNT #1 is measured as 1.4 eV, yielding a diameter of 0.55 nm, which is substantially less than the measured height of this structure. This, and the lack of order in the coating implies that SWNT #1 is not a single coated SWNT but a rope of a small number of low diameter SWNT coated with PmPV. This is supported by the strong helicity in this structure, which appears to be two, or possibly more, intertwined SWNT. This is confirmed by observing the lower part of the figure, where the rope breaks into two parts with the substrate apparent between them.

This is further confirmed by noting that the LDOS of SWNT #1 is much less well defined, with the van Hove singularities being weaker and broader than in SWNT #2. This can be explained by the fact that the tunneling current has less electrical contact to the substrate, having to pass through two or possibly more SWNT. This will reduce the tunneling current, and probably induce broadening, depending on the local intertubule interaction, and the electronic structure of the other nanotubes, which may be of a different chirality, and thus have van Hove singularities at different energies.

3.3. Spectroscopy. Additionally, PmPV−nanotube composites have been characterized by spectroscopic methods to examine the effect of the interaction with the nanotubes on the PmPV. Shown in Figure 6 is the absorption spectrum of the composite, with reference spectra of the pure PmPV and SWNT for comparison. Due to variation in sample conditions, the intensity of the measured spectrum of the composite differs to that of the pure PmPV, and so both are normalized to the lowest energy peak at ∼3 eV. In this region, the absorption of SWNT is relatively featureless, exhibiting a broad plasmon resonance throughout the spectrum, with a maximum at approximately 5 eV.[31] This resonance dominates the spectrum masking the expected contribution from the van Hove singularities. It is included here to demonstrate that features in the composite spectrum are not due to a simple superposition of components, but due to modification of the PmPV spectrum by the introduction of nanotubes.

The low energy spectrum is dominated by two well-defined peaks at 2.98 eV and at 3.69 eV. The low energy peak at 2.98 eV is due to transitions between states delocalized along the PmPV backbone.[32] The state at 3.69 eV has been assigned to the effects of broken charge conjugation symmetry in substituted PPV derivatives.[33] There are three poorly resolved features in the higher order (>4.5 eV) region, at 4.98 eV, 5.45 eV, and 6.0 eV. These are due to localized excitations of the electrons on the phenyl ring.[34]

When comparing the absorption of the SWNT/PmPV composite to the pure polymer, it is immediately noticeable that there are many dramatic differences. The low energy peak has blue-shifted from 3 eV in the polymer to 3.15 eV in the composite. This is consistent with a substantial reduction in electron delocalization along the chain, due to the curvature

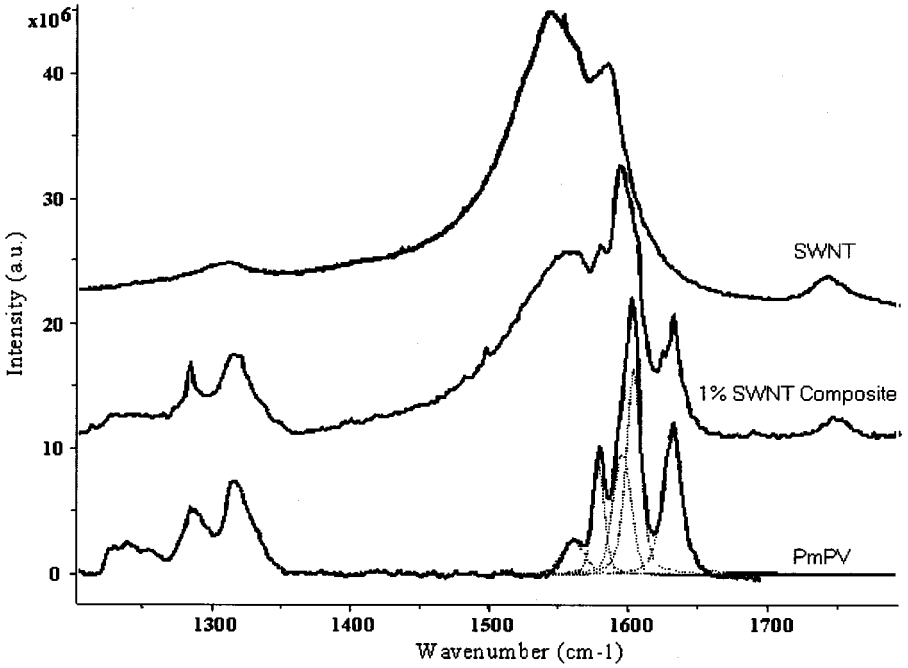

Figure 7. Raman spectrum of composite, with PmPV and SWNT spectra for comparison. From top to bottom are the SWNT spectrum, the composite spectrum, and the PmPV spectrum, respectively.

imposed as it binds onto the cylindrical substrate provided by the nanotube. This has been previously suggested by Ago et al.,[35] and modeling and microscopic evidence for this is presented here. The 3.7 eV PmPV peak, upon introduction of the SWNT, splits into two features—3.64 eV and 4.0 eV. These are also noticeably stronger in the composite with their absorption being nearly as intense as the 3 eV peak in contrast to the pure PmPV. As the original peak is due to broken charge conjugation symmetry in the PmPV, this suggests that the symmetry is further broken due to the resultant curvature imposed on the PmPV conformation by the presence of the SWNT.

Raman scattering is a powerful technique to probe the structure−property relationship in both carbon nanotubes and conjugated polymers. In Figure 7, the high frequency region of the PmPV spectrum is compared to that of the composite for an excitation wavelength of 676 nm. For completeness, the spectrum of nanotube powder is also shown. In this region, the so-called G-line feature centered at 1580 cm^{-1} dominates the nanotube spectrum. This group of modes corresponds to splitting of the optical phonon, the $E2_g$ mode in graphite, into longitudinal components at high energies and transverse ones at lower energies. The apparent broadening on the low frequency side has been attributed to both metallic and semiconducting nanotubes being resonant at this excitation energy.[31]

In this region, the spectrum of the polymer is dominated by a multiplet of modes centered on 1600 cm^{-1}. The spectrum is fitted by searching the minimum number of frequencies that fitted the different Raman bands equally well without fixing the positions and the widths of the individual peaks. The band at 1627 cm^{-1} can be attributed mainly to the vinyl group A_g mode (stretching of C═C bond).[36,37] The other bands may be attributed mainly to the phenyl group A_g mode (stretching of C−C bond). There are also a number of features centered at 1300 cm^{-1}. In PPV, the main band at 1330 cm^{-1} has been assigned to a vibration associated with the vinyl bond. In the composite, the introduction of nanotubes causes a number of modifications to the spectrum. The broad band at 1627 cm^{-1} appears to evolve into two well-defined features. There also

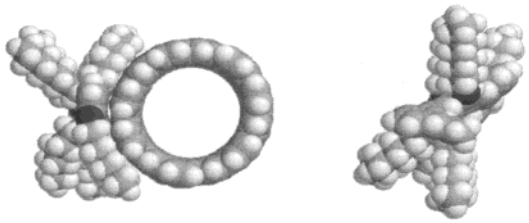

Figure 8. Modeling of PmPV−SWNT interacting. The polymer conformation can be seen to change dramatically due to the interaction with the nanotube lattice.

appear to be modifications to the relative intensities of the modes at 1610 cm^{-1} and 1590 cm^{-1}. This change manifests itself as the 1590 cm^{-1} band becoming dominant. These changes cannot be explained by a superposition of modes due to the different species, indicating that the vibrational structure of the polymer is being altered due the binding onto the SWNT lattice. These observations agree well with the microscopic observations of PmPV−SWNT interactions, and support the hypothesis that polymer conformation is strongly modified by its interaction with the nanotube.

3.4. Modeling and Simulation. Atomistic molecular dynamics simulations[38] using the COMPASS force field[39] have been employed to clarify the nature of these observed effects. Figure 8 compares a short-chain (4 repeat units) PmPV in its non-interacting conformation[40] to that when it is bound onto a (12,7) SWNT, as observed by STM. Immediately noticeable is that SWNT−PmPV interaction substantially changes the conformation of the PmPV. The PmPV backbone has curvature imposed upon it, and the sidegroups are bound onto the cylindrical substrate provided by the SWNT.

4. Discussion

Composite materials based on PmPV and various types of carbon nanotubes have been examined by TEM, STM, and optical and Raman spectroscopy. TEM investigations demonstrate a good interaction between the PmPV and nanotubes, as the nanotubes are coated heavily with PmPV. This wetting is

sufficient to enable dispersion of the polymer-coated nanotubes in common organic solvents, while nanotubes alone are insoluble in all known solvents. Of further interest are the occasional observations of dendritic growth nucleated from the nanotube lattice. Most frequently, these are observed from the tips of the nanotubes, but in some unusual cases are observed nucleating from the walls of the nanotubes. It is apparent that nanotube defects nucleate crystalline growth. This is suggested for a number of reasons. These growths are most commonly observed from the tips, where it is known that defects, e.g., pentagons, are typically found, inducing closure of the nanotube. In the cases where the nanotube tips are visible, there is good correspondence between the crystalline growths and the points of sharpest curvature, where defects most probably lie. They are only observed growing from the walls of nanotubes in catalytically grown samples, where defects are much more common. There is also an excellent correspondence between those growths and kinks in the nanotubes, which again indicate the presence of defects. Toward the tip of the nanotubes, these growths become much more numerous, and while kinks are not that apparent in this region, studies elsewhere[41] have demonstrated that defects likewise become much more frequent toward the tips of catalytically grown nanotubes.

These growths are not always observed at the tips of carbon nanotubes, although defects are always present, and so the presence of defects alone is not sufficient to account for these. PmPV has a crystalline nature, and so it is likely that the slow precipitation of PmPV from solution is necessary for these to form. These form as the solution dries on the TEM grid, as the solvent evaporates and the solution becomes super-saturated. Therefore, these growths would only form during the initial stages of evaporation, when the rate of precipitation is low, and such order would not arise as the precipitation rate increases as the solvent evaporates.

TEM of SWNT composites demonstrates similar excellent wetting between the nanotube lattice and the PmPV, with ropes of SWNT (diameter ~6 nm) being coated with approximately 30−50 nm of PmPV. Additionally, in some rare cases, an obvious symmetry is observed in the coating of the PmPV over a large range, extending over the observable length of the nanotube, about 500 nm. This coating is cylindrically symmetric, but inclined at a slight angle to the cylindrical axis of the nanotube. This is measured at approximately $7 \pm 2°$. Remarkably, this is also observed when examining similar composites by STM, but over a much smaller scale. In TEM, this ordered coating is observed to vary between 40 and 100 nm in diameter over the length of the SWNT, while in STM it has a diameter of approximately 2 nm. This large range of diameters observed in these structures demonstrates that this ordered binding of PmPV to SWNT is propagated through subsequently deposited layers, due to its crystalline nature,[20] and reflected in these layers. Also of interest is the STM observation showing the angle between the cylindrical axis and the coating symmetry much different to the $19 \pm 2°$ observed by TEM. This variance in symmetry, and the lack of correspondence to the cylindrical axis of the coating, is interesting as it indicates that the order is not determined by the coating, but rather of some underlying symmetry in the system, i.e., the lattice structure of the SWNT. Analyzing the electronic structure of this ordered structure shows that only one SWNT lies within, with a diameter of 1.3 nm, supporting this hypothesis.

This is further confirmed by contrasting these observations of order with another SWNT structure, SWNT #1, which does not have any symmetry to its coating. The electronic structure demonstrates that a rope of SWNT lies within, which would lack any underlying symmetry for PmPV to map onto. Again, comparing this to the fibers observed by TEM which lack symmetry, it can be seen that in some cases, the ropes which lie within can be observed, confirming that the observed lack of order is indicative of SWNT ropes.

The interaction binding PmPV onto nanotubes is also observed in the substantial modifications of the optical and vibrational spectroscopy of the PmPV. The absorption spectrum of the composite indicates a significant reduction in electron delocalization as compared with the pure PmPV. This result strongly suggests significant alteration of chain conformation due to nanotube interaction. These changes are mirrored in the Raman spectroscopy, where it can be seen that there are substantial differences with a much greater resolution in the spectrum. This is consistent with a reduction in the vibrational freedom of the PmPV due to its binding interaction with the nanotubes.

Modeling of the PmPV−SWNT system demonstrates the reasons for the substantial spectroscopic changes in the composite. Spectroscopic results are all consistent with the premise that the electron delocalization along the polymer chain in the composite is much less than in the pure PmPV, as would be the case if the backbone conformation is modified due to its interaction with a SWNT. The sidegroups are observed to distort the polymer conformation as they bind onto the nanotube lattice, inducing curvature in the PmPV backbone, and thus reducing electron delocalization, as observed spectroscopically. This also demonstrates the increased symmetry breaking observed spectroscopically. The PmPV is demonstrated to preferentially align itself along the SWNT cylindrical axis, interacting with the SWNT by means of $\pi-\pi$ stacking onto the SWNT lattice. While this suggests that the polymer does not map to the hexagonal lattice, this may be due to limitations in the computer model. In general the exposed relatively flat PmPV backbone[40] may be assumed to play an important role in facilitating $\pi-\pi$ stacking.

5. Conclusions

An interesting interaction between carbon nanotubes and a conjugated polymer has been observed and characterized. This manifests itself in a number of ways, i.e., good wetting between the polymer and nanotubes, the nucleation of crystalline growth by defects in the nanotubes, and a structured wrapping of the polymer onto the nanotube lattice. Spectroscopic analysis of this composite material demonstrates that the interaction results in significant changes in the properties, indicating a substantial reduction in electron delocalization, and much less vibrational freedom of the polymer. This agrees well with the observations of polymer−nanotube binding. Modeling of the interaction indicates that the polymer conformation is changed dramatically due to the interaction, in ways consistent with the spectroscopic analysis.

A similar effect has been observed in the self-ordering of proteins onto carbon nanotubes,[42] but not previously in nonbiological materials useful for device applications, such as conjugated polymers. Due to the good wetting of the nanotubes by the polymer, this suggests an accessible way to incorporate the desirable properties of nanotubes, such as mechanical reinforcement and high conductivity, into device applications. Also, the possibility of modifying and enhancing the optoelectronic properties of conjugated polymers by nonchemical means is suggested.

Acknowledgment. The authors thank the Irish Higher Education Authority and the European Union for funding. We thank the Trinity College Electron Microscopy Unit for use of their facilities.

References and Notes

(1) Iijima, S. *Nature* **1991**, *354*, 56.
(2) Tans, S. J.; Devoret, M. H.; Dai, H.; Thess, A.; Smalley, R. E.; Geerligs, L. J.; Dekker, C. *Nature* **1997**, *386*, 474.
(3) Dai, H.; Hafner, J. H.; Rinzler, A. G.; Colbert, D. T.; Smalley, R. E. *Nature* **1996**, *384*, 147.
(4) Sander, S. J.; Tans, J.; Verschueren, A. R. M.; Dekker, C. *Nature* **1998**, *393*, 49.
(5) Treacy, M. M. J.; Ebbesen, T. W.; Gibson, J. M. *Nature* **1996**, *381*, 678.
(6) Wildoer, J. W. G.; Venema, L. C.; Rinzler, A. G.; Smalley, R. E.; Dekker, C. *Nature* **1998**, *391*, 59.
(7) Odom, T. W.; Huang, J.; Kim, P.; Lieber, C. M. *Nature* **1998**, *391*, 62.
(8) Tang, B. Z.; Xu, H. Y. *Macromolecules* **1999**, *32*, 2569.
(9) Jin, Z.; Pramoda, K. P.; Xu, G.; Goh, S. H. *Chem. Phys. Lett.* **2001**, *337*, 43.
(10) Hwang, G. L.; Hwang, K. C. *J. Mater. Chem.* **2001**, *11*, 1722.
(11) Dong, S. R.; Tu, J. P.; Zhang, X. B. *Mater. Sci. Eng. A* **2001**, *313*, 83.
(12) Curran, S.; Ajayan, P. M.; Blau, W.; Carroll, D. L.; Coleman, J. N.; Dalton, A. B.; Davey, A. P.; Drury, A.; McCarthy, B.; Maier, S.; Strevens, A. *Adv. Mater.* **1998**, *10*, 1091.
(13) Friend, R. H.; Gymer, R. W.; Holmes, A. B.; Burroughes, J. H.; Marks, R. N.; Taliani, C.; Bradley, D. D. C.; Santos, D. A. D.; Brédas, J. L.; Lögdlund, M.; Salaneck, W. R. *Nature* **1999**, *397*, 121.
(14) Fournet, P.; Coleman, J. N.; O'Brien, D. F.; Lahr, B.; Drury, A.; Hörhold, H.-H.; Blau, W. J. *J. Appl. Phys.* **2001**, *90*, 969.
(15) Ajayan, P. M.; Schadler, L. S.; Giannaris, C.; Rubio, A. *Adv. Mater.* **2000**, *12*, 750.
(16) Coleman, J. N.; Dalton, A. B.; Curran, S.; Rubio, A.; Davey, A. P.; Drury, A.; McCarthy, B.; Lahr, B.; Ajayan, P. M.; Roth, S.; Barklie, R. C.; Blau, W. J. *Adv. Mater.* **2000**, *12*, 213.
(17) Murphy, R. J.; Coleman, J. N.; Cadek, M.; McCarthy, B.; Bent, M.; Drury, A.; Barklie, R. C.; Blau, W. J. *J. Chem. Phys. B.*, submitted.
(18) Duesberg, G. S.; Burghard, M.; Muster, J.; Philipp, G.; Roth, S. *Chem. Commun.* **1998**, 435.
(19) Ebbesen, T. W.; Ajayan, P. M.; Hiura, H.; Tanigaki, K. *Nature* **1994**, *367*, 519.
(20) Resel, R.; Tertinek, B.; Tasch, S.; Davey, A. P.; Blau, W.; Horhold, H.; Rost, H.; Leising, G. *Synth. Met.* **1999**, *101*, 96.
(21) Cadek, M.; Murphy, R.; McCarthy, B.; Lahr, B.; Panhuis, M. i. h.; Coleman, J. N.; Barklie, R. C.; Blau, W. J. *Carbon*, *t*o be published.
(22) Krätschmer, W.; Lamb, L. D.; Fostiropoulos, K.; Huffman, D. R. *Nature* **1990**, *347*, 354.
(23) Journet, C.; Maser, W. K.; Bernier, P.; Loiseau, A.; Chapelle, M. L. d. l.; Lefrant, S.; Deniard, P.; Lee, R.; Fischer, J. E. *Nature* **1997**, *388*, 756.
(24) Fonseca, A.; Hernadi, K.; Piedigrosso, P.; Colomer, J.-F.; Mukhopadhyay, K.; Doome, R.; Lazarescu, S.; Biro, L. P.; Lambin, P.; Thiry, P. A.; Bernaerts, D.; Nagy, J. B. *Appl. Phys. A* **1998**, *67*, 11.
(25) Lambin, P.; Fonseca, A.; Vigneron, J. P.; Nagy, J. B.; Lucas, A. A. *Chem. Phys. Lett.* **1995**, *245*, 85.
(26) Clemmer, C. R.; Beebe, T. P. *Science* **1991**, *251*, 640.
(27) Chiang, H.; Bard, A. J. *Langmuir* **1991**, *7*, 1143.
(28) van Hutten, P. F.; Brouwer, H. J.; Krasnikov, V. V.; Ouali, L.; Stalmach, U.; Hadziioannou, G. *Synth. Met.* **1999**, *102*, 1443.
(29) Dresselhaus, M. S.; Dresselhaus, G.; Eklund, P. C. *Science of Fullerenes and Carbon Nanotubes*; Academic Press: New York, 1996.
(30) Lane, P. A.; Wei, X.; Vardeny, Z. V. *Phys. Rev. Lett.* **1996**, *77*, 1544.
(31) Kataura, H.; Kumazawa, Y.; Maniwa, Y.; Umezu, I.; Suzuki, S.; Ohtsuka, Y.; Achidsfba, Y. *Synth. Met.* **1999**, *103*, 2555.
(32) Mellor, H.; Bleyer, A.; Bradley, D. D. C.; Lane, P. A.; Martin, S. J.; Rohlfing, F.; Tajbakhsh, A. *SPIE* **1997**, *382*, 3145.
(33) Gartstein, Y. N.; Rice, M. J.; Conwell, E. M. *Phys. Rev. B* **1995**, *51*, 5546.
(34) Beljonne, D.; Shuai, Z.; Cornil, J.; Santos, D. A. d.; Bredas, J. L. *J. Chem. Phys.* **1999**, *111*, 2829.
(35) Ago, H.; Schaffer, M. S. P.; Ginger, D. S.; Windle, A. H.; Friend, R. H. *Phys. Rev. B* **2000**, *61*, 2286.
(36) Sakamoto, A.; Furukawa, Y.; Tasumi, M. *J. Phys. Chem.* **1992**, *96*, 1490.
(37) Lefrant, S.; Perrin, E.; Buisson, J. P.; Eckhardt, H.; Han, C. C. *Synth. Met.* **1989**, *29*, E91.
(38) Cerius 2 Software, Accelrys Inc., 9685 Scranton Road, San Diego, CA 92121-3752.
(39) Sun, H.; Rigby, D. *Spectrochim. Acta A* **1997**, *53*, 1301.
(40) in het Panhuis, M.; Munn, R. W.; Blau, W. J. *Synth. Met.* **2001**, *121*, 1187.
(41) Endo, M.; Takeuchi, K.; Igarashi, S.; Kobori, K.; Shirasishi, M.; Kroto, H. W. *J. Phys. Chem. Solids* **1993**, *54*, 277.
(42) Balavoine, F.; Schultz, P.; Richard, C.; Mallouh, V.; Ebbesen, T. W.; Mioskowski, C. *Angew. Chem., Int. Ed.* **2000**, *38*, 1919.